NOTES AND CORRESPONDENCE

Estimating the Decadal Predictability of a Coupled AOGCM

HOLGER POHLMANN AND MICHAEL BOTZET

Max-Planck-Institut für Meteorologie, Hamburg, Germany

MOJIB LATIF

Leibniz-Institut für Meereswissenschaften, Universität Kiel, Kiel, Germany

ANDREAS ROESCH, MARTIN WILD, AND PETER TSCHUCK

Institut für Atmosphäre und Klima, Eidgenössische Technische Hochschule, Zürich, Switzerland

4 December 2003 and 14 May 2004

ABSTRACT

On seasonal time scales, ENSO prediction has become feasible in an operational framework in recent years. On decadal to multidecadal time scales, the variability of the oceanic circulation is assumed to provide a potential for climate prediction. To investigate the decadal predictability of the coupled atmosphere–ocean general circulation model (AOGCM) European Centre-Hamburg model version 5/Max Planck Institute Ocean Model (ECHAM5/MPI-OM), a 500-yr-long control integration and ''perfect model'' predictability experiments are analyzed. The results show that the sea surface temperatures (SSTs) of the North Atlantic, Nordic Seas, and Southern Ocean exhibit predictability on multidecadal time scales. Over the ocean, the predictability of surface air temperature (SAT) is very similar to that of SST. Over land, there is little evidence of decadal predictability of SAT except for some small maritime-influenced regions of Europe. The AOGCM produces predictable signals in lower-tropospheric temperature and precipitation over the North Atlantic, but not in sea level pressure.

1. Introduction

In the field of climate prediction, great progress has been attained with the ability to predict the El Niño–Southern Oscillation (ENSO) phenomenon (e.g., Latif et al. 1994, 1998). El Niño, the irregular warming of sea surface temperature (SST) in the equatorial east Pacific, coincides with the negative phase of the Southern Oscillation, a seesaw in sea level pressure (SLP) between southeast Asia and the eastern Pacific region. The coupled atmosphere–ocean phenomenon ENSO is the most important climate mode on seasonal to interannual time scales, causing various climate disturbances around the globe. A comprehensive in situ observation system of the equatorial Pacific forms, together with satellite measurements, the basis for ENSO predictions. ENSO predictions are performed routinely by a number of prediction centers using statistical methods and coupled atmosphere–ocean general circulation models (AOGCMs). Recent findings on this topic are published in the *Experimental Long-Lead Forecast Bulletin* (available online at http://grads.iges.org/ellfb).

The thermohaline circulation (THC), a component of the global ocean circulation, is driven by differences in the density of seawater, which is controlled by temperature and salinity. In regions of the Labrador and Nordic Seas and in the Southern Ocean around Antarctica, surface water is cooled and sinks into the deep ocean. Surface currents replace the water masses and transport heat poleward (Trenberth and Caron 2001). In the Atlantic, this poleward heat transport contributes to a milder European winter climate than without these currents (Broecker 1991). However, Seager et al. (2002) criticize the responsibility of these heat transports for European's mild winters and argue that the oceanic heat storage and atmospheric heat transport are important. The discussion of the relative importance of the oceanic heat and salt transports for European climate is ongoing (Rhines and Häkkinen 2003). The THC varies on multidecadal time scales (Dickson et al. 1996; Timmermann et al. 1998; Delworth and Mann 2000). The predictability attributed to this climate variability is investigated in this study using an AOGCM.

Corresponding author address: Holger Pohlmann, Max-Planck-Institut für Meteorologie, Bundesstr. 53, D-20146 Hamburg, Germany.
E-mail: holger.pohlmann@dkrz.de

Decadal predictability is estimated by diagnostic and prognostic approaches. In the diagnostic approach, the predictability is analyzed by decomposing the variance of a climate variable into a long time scale potentially predictable component and an unpredictable noise component. The diagnostic potential predictability of the Canadian Centre for Climate Modelling and Analysis (CCCma) AOGCM is estimated in the study of Boer (2000) and that of a multimodel ensemble is estimated in the studies of Boer (2001, 2004). Potential predictability is found in the multimodel studies predominantly in the high latitude oceans, with appreciable values on multidecadal time scales especially in the Southern Ocean and the North Atlantic. In the prognostic approach, the predictability is estimated with ''perfect model'' AOGCM experiments. Starting from identical oceanic and perturbed atmospheric initial conditions, ensemble experiments are performed. The spread within the ensemble is interpreted as an estimate of predictability. The use of identical oceanic initial conditions implies the assumption that the AOGCM could be perfectly initialized with three-dimensional oceanic observational fields. Thus, since this is not possible, this technique gives an upper limit of predictability. Using the Geophysical Fluid Dynamics Laboratory (GFDL) model, Griffies and Bryan (1997a,b) found that in the North Atlantic region the first empirical orthogonal function (EOF) of the dynamical sea surface topography is predictable up to 10–20 yr on average, and SST in the East Greenland Sea is predictable 5–15 yr in advance. Grötzner et al. (1999) used the European Centre-Hamburg model version 3/Large-Scale Geostropic (ECHAM3/LSG) model and found that the North Atlantic THC is predictable about one decade in advance, but North Atlantic SST is only predictable about 1 yr in advance. Boer (2000) analyzed simulations with the CCCma model and found predictable surface air temperatures (SATs) on multidecadal time scales mainly in the Southern Ocean. Collins (2002) used the third Hadley Centre Coupled Ocean–Atmosphere GCM (HadCM3) and found that SAT in the North Atlantic region is predictable on decadal time scales. Collins and Sinha (2003) have shown some indication that the multidecadal THC predictability in HadCM3 leads to weak but significant predictability of western European climate.

These studies and the recent predictability comparison of Collins et al. (2003) show that the predictability of oceanic and atmospheric components depends strongly on the model formulation. However, the possibilities of decadal climate predictability with AOGCMs are unclear since the number of decadal predictability studies is limited. The AOGCM experiments of this study exhibit relatively high predictabilities and therefore may reveal new chances for climate prediction. The remainder of this paper is organized as follows: The AOGCM and the experiments used in this study are described in section 2. The concepts of diagnostic and prognostic potential predictability are introduced in section 3 and are applied to estimate the climate predictability of our AOGCM in section 4. Section 5 concludes this paper with a summary and discussion of the results.

2. Model and experiments

The model used in this study is the global coupled ECHAM5/Max Planck Institute Ocean Model (MPI-OM). The atmospheric component, ECHAM5 (version 5.0; Roeckner et al. 2003), is run at T42 resolution, which corresponds to a horizontal resolution of about $2.8° \times 2.8°$. The oceanic component, MPI-OM (Marsland et al. 2003), is based on a C-grid version of the Hamburg Ocean Primitive Equation (HOPE) ocean model. It is run on a curvilinear grid with equatorial refinement. A dynamic/thermodynamic sea ice model (see also Marsland et al. 2003) and a hydrological discharge model (Hagemann and Dümenil Gates 2001) are included in this model. The atmospheric and oceanic components are coupled with the Ocean Atmosphere Sea Ice Soil (OASIS) coupler (Terray et al. 1998). The model does not employ flux adjustment or any other corrections.

A 500-yr-long control integration of ECHAM5/MPI-OM, in which the concentrations of the greenhouse gases are fixed to the values of the 1990s, is used to estimate the low-frequency climate variability. The first 50 yr of the control integration are not considered in order to allow for the spinup of the coupled system. The North Atlantic THC of this integration exhibits strong multidecadal variations (Latif et al. 2004). From the control integration, three different years (90, 125, and 170), corresponding to intermediate, strong, and weak North Atlantic THC conditions, are selected and used as initial conditions for three ensemble experiments. Each ensemble consists of six experiments realized with slightly perturbed atmospheric, but the same oceanic, initial conditions. The experiments cover a 20-yr-long integration period. These ensemble experiments are referred to as predictability experiments.

3. Methods

This study is idealized, since no observational data for the initialization of the experiments or the verification of the results are used. Instead, the upper predictability limit of ECHAM5/MPI-OM is estimated by applying the methods of ''prognostic potential predictability'' (PPP) and ''diagnostic potential predictability'' (DPP). For the prognostic predictability approach we perform perfect model ensemble experiments with the AOGCM ECHAM5/MPI-OM, while the 500-yr-long control integration with this AOGCM is analyzed in the diagnostic predictability approach.

a. Diagnostic potential predictability

The method of analysis of variances (Madden 1976; Rowell 1998) is applied to investigate the variability of

our control integration. To distinguish this method from the prognostic approach introduced in the next section, we call it diagnostic potential predictability. DPP attempts to quantify the fraction of long-term variability that may be distinguished from the internally generated natural variability, which is not predictable on long time scales and so may be considered as noise. For this concept the variance of some mean quantity is investigated to determine whether it is greater than can be accounted for by sampling error given the noise in the system. The variances of a certain climate variable from the control integration (of length $l = nm$) are estimated from the m-year means (σ_v^2) and the average of the deviations of the annual means from them (σ_ε^2). In a first step, we test the null hypothesis that the data are independent random variables, which possess no long time-scale potential predictability. Following Boer (2004), the null hypothesis is rejected using an F test (e.g., von Storch and Zwiers 1999) if

$$\frac{(m-1)\sigma_v^2}{\sigma_\varepsilon^2} > \mathrm{F}_{n-1,n(m-1)}. \tag{1}$$

As noted in Rowell (1998), the one-sided test, which is not affected by serial correlation in the data, has to be used. In a second step, DPP is calculated. As Boer (2004) shows, it can be derived in two ways resulting in two different estimates for DPP. We use the more conservative estimate here:

$$\mathrm{DPP} = \frac{\sigma_v^2 - \frac{1}{m}\sigma^2}{\sigma^2}, \tag{2}$$

where $\sigma^2 = \sigma_v^2 + \sigma_\varepsilon^2$ is the total variance. The longer time-scale variance is discounted in this equation to account for the fact that short-term noise contributes to the calculated long time-scale variance.

b. Prognostic potential predictability

The ensemble spread (ensemble variance) of a climate variable X from the ensemble experiments in relation to its variance in the control integration (σ^2) gives a measure for the PPP. Here, PPP (as a function of the prediction period t) is defined as the average over all ensemble experiments:

$$\mathrm{PPP}(t) = 1 - \frac{\frac{1}{N(M-1)}\sum_{j=1}^{N}\sum_{i=1}^{M}[X_{ij}(t) - \overline{X}_j(t)]^2}{\sigma^2}, \tag{3}$$

where X_{ij} is the ith member of the jth ensemble, $\overline{X}_j$ is the jth ensemble mean, and N (M) is the number of ensembles (ensemble members). In this study, each of the three experiments ($N = 3$) consists of six ensemble members and the control integration ($M = 7$), which is regarded as an additional ensemble member. PPP amounts to a value of 1 for perfect predictability and a value of 0 for an ensemble spread equal to the variance of the control integration. The significance of PPP is estimated, determining if the ensemble variance is different to the variance of the control integration. The F test is used for this decision; that is, if

$$\mathrm{PPP}(t) > 1 - \frac{1}{\mathrm{F}_{N(M-1),k-1}}, \tag{4}$$

where the degrees of freedom of the control integration (k) are reduced with the concept of the decorrelation time for a first-order autoregressive (AR-1) process [Eq. (17.11) in von Storch and Zwiers (1999)].

The results are compared with the statistical climate prediction concept of ''damped persistence.'' This statistical forecast method takes into account the climatological mean and the damping coefficient estimated from the history of the system. It is based on the concept of Hasselmann's (1976) stochastic climate model. In this model, the system is divided into a fast (atmosphere) and a slow (ocean) component. In the mathematical formulation of the slow processes, atmospheric variability (weather) is treated as ''noise,'' which is integrated by the ocean resulting in low-frequency variability. The differential equation describing this AR-1 process is given by

$$\frac{dX(t)}{dt} = -\alpha X(t) + Z(t), \tag{5}$$

where α is the damping coefficient and $Z(t)$ is a random variable with Gaussian characteristics. The average of several realizations of Eq. (3), that is, the noise-free solution, is

$$\overline{X}(t) = X_{\mathrm{clim}} + X_0 e^{-\alpha t}. \tag{6}$$

This equation describes the averaged damping from an initial anomaly X_0 toward the climatological mean X_{clim}. The prognostic potential predictability of a hypothetical ensemble generated by stochastic processes is given by [see Eq. (8) of Griffies and Bryan (1997b)]

$$\mathrm{PPP}(t) = e^{-2\alpha t}. \tag{7}$$

When the damping coefficient is small, the prognostic potential predictability is high, and a prediction with this statistical method is reasonable.

4. Results

a. Climate variability

Analyzing the ECHAM5/MPI-OM control integration, Latif et al. (2004) found a close relationship between variations of the North Atlantic THC, defined as the maximum of the meridional overturning circulation (MOC) at 30°N (i.e., the maximum in the North Atlantic in the control integration), and SST averaged over the region 40°–60°N, 50°–10°W. Figure 1a shows the linear correlation between decadal means of the North Atlantic

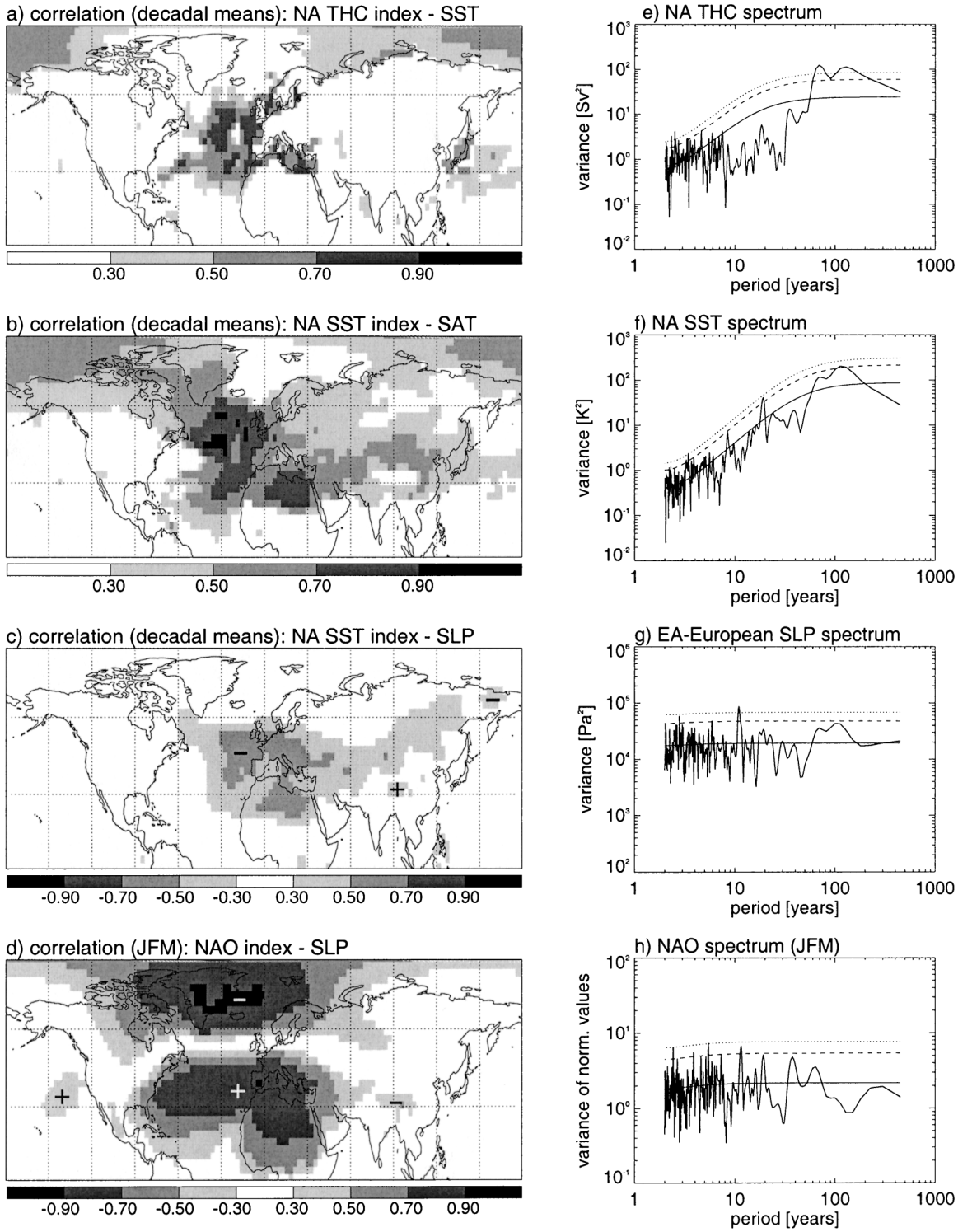

FIG. 1. Analyses of the climate variability in the control integration. Correlation maps between the (a) North Atlantic THC index and SST; (b) North Atlantic SST index and SAT, and (c) North Atlantic SST index and SLP; and (d) NAO index and SLP. (a)–(c) Based on decadal means. The shaded values are significant on the 95% significance level according to a *t* test. (d) Based on winter (JFM) means. Only positive values are plotted in (a) and (b), and in (c) and (d) the sign of the correlation is marked. Also shown are the spectra of time series for the (e) North Atlantic THC, (f) North Atlantic SST, (g) east Atlantic–European SLP, and (h) NAO. (e)–(g) are based on annual means and (h) is based on winter (JFM) means. Additionally shown in (e)–(h) are the spectra of fitted AR-1 processes (solid), and the 95% (dashed) and 99% (dotted) significance levels according to these processes.

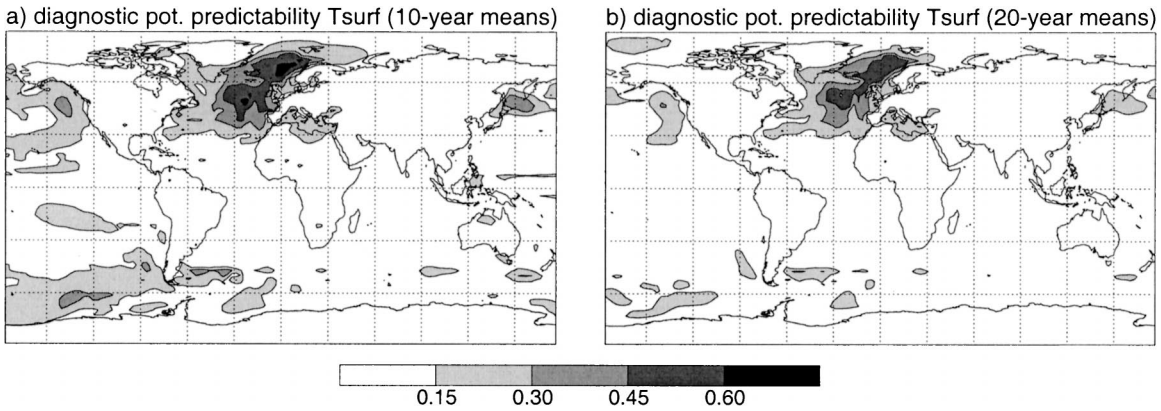

FIG. 2. Diagnostic potential predictability of surface temperature (Tsurf) based on (a) 10-yr means and (b) 20-yr means. The shaded values are significant at the 99% significance level according to an F test.

THC (maximum MOC at 30°N) and SST over the Northern Hemisphere. Temporal dependence of the data is taken into consideration for statistical tests of the significance of the correlation values reducing the degrees of freedom with the concept of the decorrelation time for an AR-1 process [Eq. (17.11) in von Storch and Zwiers (1999)]. Strongest (positive) correlations exist in the central North Atlantic region. Therefore the same North Atlantic SST index as in Latif et al. (2004) is used to investigate the relation to the atmospheric variables SAT and SLP. Figure 1b shows the correlation values between decadal means of the North Atlantic SST index and SAT. Significant positive correlation values exist nearly over the whole North Atlantic, extending also over Europe and Asia. Figure 1c shows the correlation values between decadal means of the North Atlantic SST index and SLP. The correlation pattern is a monopole with significant (negative) correlation values over the east Atlantic and Europe. Based on this analysis, we define an east Atlantic–European SLP index as the average over the region 40°–60°N, 30°W–30°E. The model simulates a realistic North Atlantic Oscillation (NAO), shown in Fig. 1d as the correlation of the NAO index with SLP in the winter season (January–February–March: JFM). The NAO index is defined as the principal component of the leading EOF of SLP in the North Atlantic–European region (15°–80°N, 90°W–40°E) for the winter season (JFM). The spatial dipole structure of the NAO is different from the monopole structure of the THC projection on the SLP field.

Spectral analyses of climate indices are shown for the North Atlantic THC (Fig. 1e), the North Atlantic SST (Fig. 1f), the east Atlantic–European SLP (Fig. 1g) and the NAO (Fig. 1h). The spectra are computed from detrended time series using a ''Bartlett'' window and two chunks. The spectra of the North Atlantic THC and SST indices are red, and those of the east Atlantic–European SLP and NAO indices are white. The North Atlantic THC spectrum shows a dominant peak at 70 yr and another peak at 100 yr, exceeding the 99% significance level. Peaks of the North Atlantic SST spectrum do not exceed the 99% significance level. The east Atlantic–European SLP spectrum exhibits a peak at 10 yr. Peaks of the NAO spectrum do not exceed the 99% significance level. Particularly, there is little amplitude of variability in the NAO on the time scales associated with the THC variability. This is different from the spectra of the ECHAM3/LSG model (Grötzner et al. 1999), which shows spectral peaks at the time scale associated with the THC both in oceanic and atmospheric quantities of the North Atlantic region.

b. Diagnostic potential predictability

Figure 2a shows the diagnostic potential predictability for decadal means of surface temperatures (i.e., SST over the oceans and land surface temperature elsewhere) of the control integration. Highest decadal DPP values exist in the North Atlantic and Nordic Seas. Other regions with high decadal DPP are present in the Southern Ocean, in the extratropical North Pacific and also in the subtropical Pacific. Our result of decadal DPP for surface temperatures shows a remarkable similarity to that of a super ensemble of nine climate models (Boer 2004). However, compared to the results of the superensemble mean, the diagnostic potential predictability of our analysis is stronger in the North Atlantic, Nordic Seas, and Pacific and weaker in the Southern Ocean, especially east of the Greenwich meridian to the date line. Figure 2b shows the diagnostic potential predictability for 20-yr means of surface temperatures. These DPP values are generally less significant than those based on 10-yr means, although considerable values remain in the North Atlantic and Nordic Seas.

c. Oceanic prognostic potential predictability

The prognostic potential predictability of surface temperatures are shown as maps averaged over the three ensemble experiments and the first and second predic-

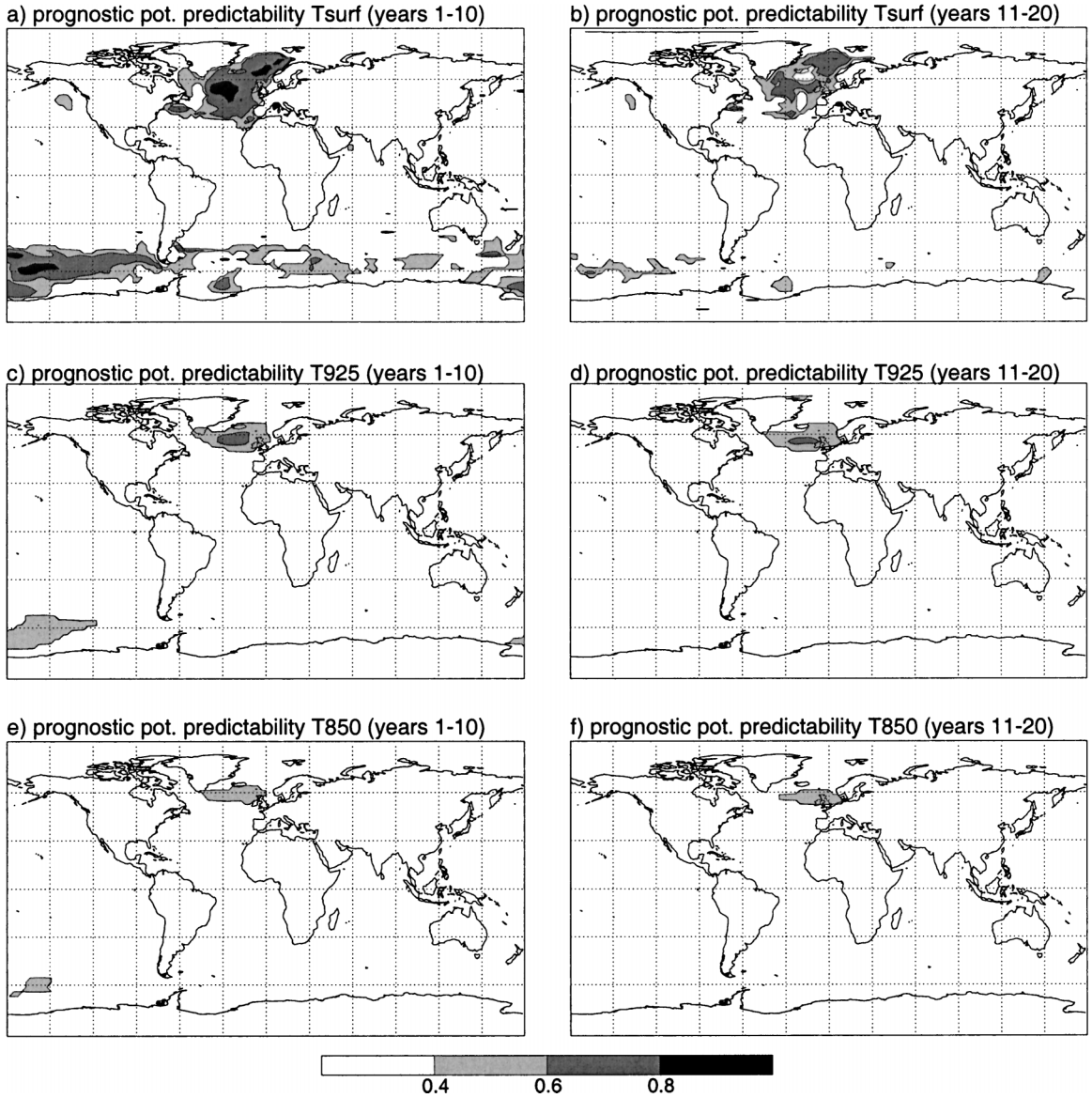

FIG. 3. PPP of temperature at (top) the surface (Tsurf), (middle) 925-hPa level (T925), and (bottom) 850-hPa level (T850) averaged over the three ensemble experiments and the (left column) first and (right column) second prediction decade. The shaded values are significant at the 90% significance level according to an F test.

tion decade in Figs. 3a and 3b, respectively. The result of this method averaged over the first decade is very similar to that of the diagnostic potential predictability method based on 10-yr means. Averaged over the first decade, the most predictable regions are in the North Atlantic, Nordic Seas, and Southern Ocean. The result of the prognostic potential predictability method averaged over the second decade is very similar to that of the diagnostic potential predictability method based on 20-yr means. The prognostic potential predictability of the second decade is everywhere less significant than that of the first decade. In this period, predictability primarily remains significant in the North Atlantic and the Nordic Seas. In these areas, the ocean exhibits multidecadal SST predictability.

SST indices are defined in regions with high predictabilities to analyze the time dependence of the predictability in more detail. An additional effect of the spatial average is an enhancement of the predictability, since small-scale fluctuations are filtered out. The time series of North Atlantic SST averaged in the region 40°–60°N, 50°–10°W of the control integration and the predictability experiments are shown together with the predictability of this SST index in Fig. 4a. The skill in predicting the North Atlantic SST index is clearly better than that of the damped persistence forecast and exceeds

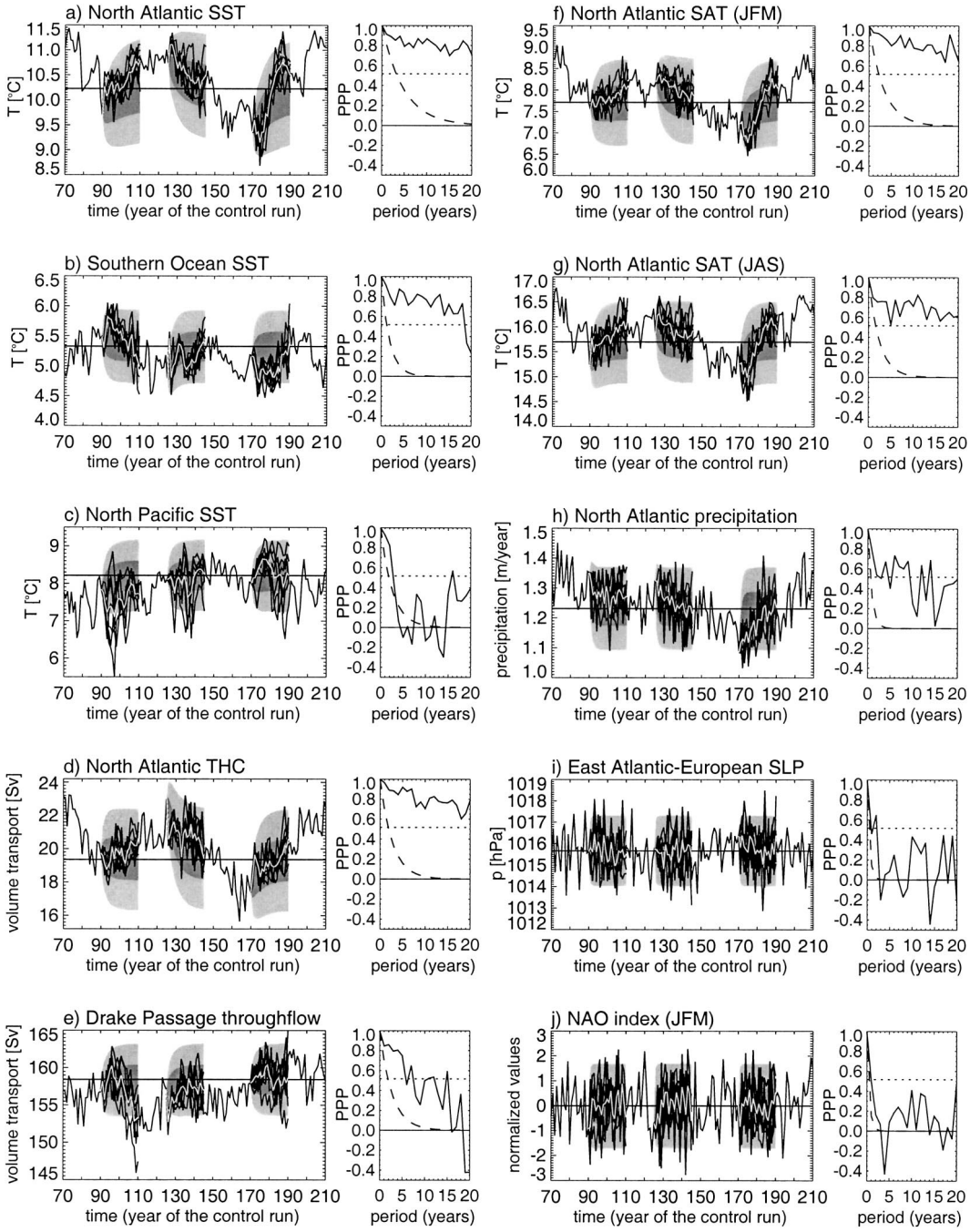

FIG. 4. (a) (left) Annual mean North Atlantic SST for years 70 to 210 of the control integration (black); ensemble forecast experiments initialized at the end of the years 90, 125, and 170 (black); and the ensemble means (white). The results of the statistical forecast method of damped persistence are shown as the range expected to contain 90% and 50% of the values from infinite size ensembles of noise driven AR-1 random processes (light and dark gray, respectively). (right) PPP of the North Atlantic SST index averaged over the three ensemble experiments (solid curve), with the damped persistence forecast (dashed) as a function of the prediction period. Additionally, the 95% significance level according to an F test is dotted. (b)–(j) As in (a), but for (b) Southern Ocean SST, (c) North Pacific SST, (d) North Atlantic THC, (e) Drake Passage throughflow, (f) North Atlantic SAT for JFM, (g) North Atlantic SAT for JAS, (h) North Atlantic precipitation, (i) east Atlantic–European SLP, and (j) the NAO index. (a)–(e) and (h)–(i) Based on annual means, (f) and (j) are based on winter (JFM) means, and (g) is based on summer (JAS) means.

the 95% significance level over the whole prediction period of 20 yr. Averaged over the first (second) prediction decade, the predictability, PPP, equals 0.86 (0.79). These values are considerably higher than the corresponding, spatially averaged predictabilities of individual grid cells as displayed in Fig. 3a (3b) of 0.61 (0.53). The time series and predictabilities of Southern Ocean SST averaged in the region 50°–60°S, 180°–80°W are shown in Fig. 4b. The skill in predicting the Southern Ocean SST index is also good and remains significant at the 95% significance level over the whole prediction period, except for the last two years. Averaged over the first (second) prediction decade, predictability equals 0.82 (0.67). These values are again considerably higher than the spatially averaged predictabilities of individual grid cells as displayed in Fig. 3a (3b) of 0.62 (0.43). Figure 4c shows the North Pacific SST averaged over the region 40°–60°N, 140°E–130°W. This SST index is much less predictable than the North Atlantic and Southern Ocean SST indices. Predictability of North Pacific SST is significant only in the first two years. Thereafter the predictability is of the order of the damped persistence forecast. Latif and Barnett (1994) found in the AOGCM ECHAM3/HOPE a coupled air–sea mode between the subtropical gyre circulation in the North Pacific and the Aleutian low pressure system from which a higher North Pacific SST predictability could be expected. The results of the diagnostic potential predictability confirm this assumption since substantial predictabilities exist in certain regions of the North Pacific (Figs. 2a and 2b). However, the prognostic potential predictability method suggests almost no significant SST predictability in these regions. A detailed analysis of the predictability in each of the three ensembles shows that the third ensemble exhibits, in contrast to the other ensembles, a significant predictability for the North Pacific SST index of about a decade. This may indicate a dependence of the North Pacific SST predictability on the initial oceanic state.

The result of the North Atlantic THC predictability analysis is shown in Fig. 4d. The skill in predicting the North Atlantic THC is significant at the 95% significance level over the whole prediction period of 20 yr and comparable to that of the North Atlantic SST. Latif et al. (2004) show the close relationship between the North Atlantic THC and SST in our AOGCM. The strength of the overturning circulation is related to the convective activity in the deep water formation regions, most notably the Labrador Sea, which is sensitive to freshwater anomalies from the Arctic (Jungclaus et al. 2004, manuscript submitted to *J. Climate*). Another region with a good skill in predicting SST exists in the Southern Ocean. The predictability of the Drake Passage throughflow (Fig. 4e) as a measure for the Antarctic Circumpolar Current (ACC) is analyzed. The predictability of the Drake Passage throughflow is clearly significant just over the first five years. This relatively short predictability period and the relatively low correlation values between ACC and Southern Ocean SST in the control integration (not shown) suggest that the strength of the ACC is not the only forcing term determining the predictability of the Southern Ocean SST.

d. Atmospheric prognostic potential predictability

The (sea and land) surface temperature and the temperature of the overlying atmosphere are closely related. Therefore the prognostic potential predictability values of SAT (not shown) are very close to the prognostic potential predictability values of the surface temperatures, which are shown in Figs. 3a and 3b. The highest PPP values of SAT exist over the North Atlantic, Nordic Seas, and Southern Ocean. Over land there is little evidence of decadal predictability of SAT except for some limited regions of maritime-influenced Europe such as Iceland, Ireland, south Greenland, parts of Great Britain, and Iberia (Figs. 3a and 3b). The predictability values of air temperature at higher levels are shown for the 925-hPa level (Figs. 3c and 3d), and the 850-hPa level (Figs. 3e and 3f). The air temperature is predictable in the lower troposphere over the Southern Ocean in the first prediction decade and over the North Atlantic in both prediction decades. The predictability of decadal mean surface relative humidity is also significant in certain regions of the North Atlantic, Nordic Seas, and Southern Ocean (not shown). However, the predictability of decadal mean SLP is not significant in the North Atlantic–European region (not shown).

Figures 4f and 4g show the time series and predictabilities for the North Atlantic SAT index defined as the average over sea points in the region 30°–65°N, 40°W–0° for winter (JFM) and summer [July–August–September (JAS)], respectively. The predictability of this index is significant at the 95% significance level over the whole prediction period in both seasons. The skill of predicting the North Atlantic SAT index is better in winter than in summer, and the variance of North Atlantic SAT is higher in winter than in summer. The atmosphere is dynamically most active in winter. As a result, it is reasonable that the atmosphere over the North Atlantic is strongest coupled to the ocean in this season. The reemergence of persistent oceanic surface anomalies in winter (Timlin et al. 2002) may also contribute to the enhanced signal in this season. Figure 4h shows the result for the North Atlantic precipitation index defined as the average over the region 50°–60°N, 40°–20°W. The North Atlantic precipitation index is significantly predictable over the first decade. Again, the predictability values of the North Atlantic SAT and precipitation are higher than the corresponding spatial averages of predictabilities at individual grid cells. A detailed analysis shows predictability of humidity to be limited to the lower troposphere. Park and Latif (2005) show that in the ECHAM5/MPI-OM AOGCM the atmospheric response to the North Atlantic decadal SST variability is shallow and that changes in the statistics

of transient eddies are not involved. Figure 4i shows the result for the east Atlantic–European SLP index and Fig. 4j shows the result for the NAO index. The NAO index is defined for the ensemble experiments as the scalar product with the leading EOF mode of the control integration based on SLP averages for the winter season (JFM). The predictabilities of these SLP-based indices are significant just in the first one or two years.

5. Summary and discussion

In this study, the decadal predictability of the coupled AOGCM ECHAM5/MPI-OM has been systematically investigated, analyzing both the control integration and the perfect model experiments. SSTs are shown to be predictable on decadal to multidecadal time scales in the North Atlantic, Nordic Seas, and Southern Ocean. Ocean dynamics is a candidate in forcing the multidecadal variability and producing the multidecadal predictability of SST. A close relationship between the North Atlantic SST and THC exists. The relation between the ACC and SST in the Southern Ocean is less clear. In addition to the decadal predictability of SST, the AOGCM produces predictable signals in the temperature of the lower troposphere. Over land there is little evidence of decadal predictability of SAT except for some limited regions of maritime-influenced Europe. Precipitation is predictable up to a decade in advance in a certain region over the North Atlantic. However, no significant decadal SLP predictability in the North Atlantic–European region has been detected, although significant correlation values between the decadal mean North Atlantic SST index and SLP exist in this region. The ''noise'' (weather) part of the atmospheric circulation overwhelms any decadal climate signal.

The decadal predictability is dependent on the model formulation. In the earlier AOGCM version, ECHAM3/LSG, the North Atlantic THC was predictable on decadal time scales, but the North Atlantic SST was not. (Grötzner et al. 1999). The higher (vertical) resolution of the oceanic component of the ECHAM5/MPI-OM AOGCM and the more realistic oceanic heat transports may be the reason of the higher SST predictability in this AOGCM. Our result of multidecadal SAT predictability is comparable with the results of the GFDL model (Griffies and Bryan 1997a,b), the CCCma model (Boer 2000), and the HadCM3 model (Collins and Sinha 2003). Furthermore, the diagnostic potential predictability in the North Atlantic is higher in ECHAM5/MPI-OM than in a superensemble of nine AOGCMs (Boer 2004). An open question is whether our AOGCM is overestimating decadal climate predictability.

In this study, the predictability problem is treated in a highly idealized manner. However, for a ''real'' climate forecast, the initial state of the three-dimensional ocean must be known. This is a big problem, since only the surface is observable with good spatial coverage by satellites. Latif et al. (2004) suggest that the relationship between variations in THC and SST can be exploited for predictability purposes, as the initial oceanic state may be derived from the history of SST. This may provide a method for determining the initial state of the ocean in order to realize predictions of multidecadal climate variability.

Acknowledgments. We thank Erich Roeckner, Johann Jungclaus, Noel Keenlyside, Ute Merkel, and the reviewers for the discussion of our results and comments on this paper. This work was supported by the European Union project PREDICATE, the German Ministry for Education and Research (BMBF) project DEKLIM, and the Swiss National Center of Competence in Climate Research (NCCR Climate). The climate simulations were conducted at the German Climate Computing Centre (DKRZ) and Swiss Center for Scientific Computing (CSCS).

REFERENCES

Boer, G. J., 2000: A study of atmosphere–ocean predictability on long time scales. *Climate Dyn.,* **16,** 469–477.

——, 2001: Decadal potential predictability in coupled models. *CLIVAR Exchanges,* No. 19, International CLIVAR Project Office, 3.

——, 2004: Long time-scale potential predictability in an ensemble of coupled climate models. *Climate Dyn.,* **23,** 29–44.

Broecker, W., 1991: The great ocean conveyor. *Oceanography,* **4,** 79–89.

Collins, M., 2002: Climate predictability on interannual to decadal time scales: The initial value problem. *Climate Dyn.,* **19,** 671–692.

——, and B. Sinha, 2003: Predictability of decadal variations in the thermohaline circulation and climate. *Geophys. Res. Lett.,* **30,** 1306, doi:10.1029/2002GL016504.

——, A. Carril, H. Drange, H. Pohlmann, R. Sutton, and L. Terray, 2003: North Atlantic decadal predictability. *CLIVAR Exchanges,* No. 28, International CLIVAR Project Office, 6–7.

Delworth, T. L., and M. E. Mann, 2000: Observed and simulated multidecadal variability in the Northern Hemisphere. *Climate Dyn.,* **16,** 661–676.

Dickson, R., J. Lazier, J. Meinecke, P. Rhines, and J. Swift, 1996: Long-term coordinated changes in the convective activity of the North Atlantic. *Progress in Oceanography,* Vol. 38, Pergamon, 241–295.

Griffies, S. M., and K. Bryan, 1997a: Predictability of North Atlantic multidecadal climate variability. *Science,* **275,** 181–184.

——, and ——, 1997b: A predictability study of simulated North Atlantic multidecadal variability. *Climate Dyn.,* **13,** 459–487.

Grötzner, A., M. Latif, A. Timmermann, and R. Voss, 1999: Interannual to decadal predictability in a coupled ocean–atmosphere general circulation model. *J. Climate,* **12,** 2607–2624.

Hagemann, S., and L. Dümenil Gates, 2001: Validation of the hydrological cycle of ECMWF and NCEP reanalyses using the MPI hydrological discharge model. *J. Geophys. Res.,* **106,** 1503–1510.

Hasselmann, K., 1976: Stochastic climate models, part 1—Theory. *Tellus,* **28,** 473–484.

Latif, M., and T. P. Barnett, 1994: Causes of decadal climate variability over the North Pacific and North America. *Science,* **266,** 634–637.

——, ——, M. A. Cane, M. Flügel, N. E. Graham, H. von Storch, J.-S. Yu, and S. E. Zebiak, 1994: A review of ENSO prediction studies. *Climate Dyn.,* **9,** 167–179.

——, and Coauthors, 1998: A review of the predictability and prediction of ENSO. *J. Geophys. Res.,* **103,** 14 375–14 393.

——, and Coauthors, 2004: Reconstructing, monitoring, and predicting multidecadal-scale changes in the North Atlantic thermohaline circulation with sea surface temperature. *J. Climate,* **17,** 1605–1614.

Madden, R. A., 1976: Estimates of the natural variability of time-averaged sea-level pressure. *Mon. Wea. Rev.,* **104,** 942–952.

Marsland, S. J., H. Haak, J. H. Jungclaus, M. Latif, and F. Röske, 2003: The Max-Planck-Institute global ocean/sea ice model with orthogonal curvilinear coordinates. *Ocean Modell.,* **5,** 91–127.

Park, W., and M. Latif, 2005: Ocean dynamics and the nature of air–sea interactions over the North Atlantic. *J. Climate,* in press.

Rhines, P. B., and S. Häkkinen, 2003: Is the oceanic heat transport in the North Atlantic irrelevant to the climate in Europe? *ASOF Newsletter,* No. 1, 13–17.

Roeckner, E., and Coauthors, 2003: The atmospheric general circulation model ECHAM5: Part I: Model description. MPI Rep. 349, Max-Planck-Institut für Meteorologie, Hamburg, Germany, 127 pp.

Rowell, D. P., 1998: Assessing the potential seasonal predicability with an ensemble of multidecadal GCM simulations. *J. Climate,* **11,** 109–120.

Seager, R., D. S. Battisti, J. Yin, N. Gordon, N. Naik, A. C. Clement, and M. A. Cane, 2002: Is the Gulf Stream responsible for Europe's mild winters? *Quart. J. Roy. Meteor. Soc.,* **128,** 2563–2586.

Terray, L., S. Valcke, and A. Piacentini, 1998: OASIS 2.2, ocean atmosphere sea ice soil, user's guide and reference manual. Tech. Rep. TR/CGMC/98-05, CERFACS, Toulouse, France, 77 pp.

Timlin, M. S., M. A. Alexander, and C. Deser, 2002: On the re-emergence of North Atlantic SST anomalies. *J. Climate,* **15,** 2707–2712.

Timmermann, A., M. Latif, R. Voss, and A. Grötzner, 1998: Northern Hemisphere interdecadal variability. *J. Climate,* **11,** 1906–1931.

Trenberth, K. E., and J. M. Caron, 2001: Estimates of meridional atmosphere and ocean heat transport. *J. Climate,* **14,** 3433–3443.

von Storch, H., and F. W. Zwiers, 1999: *Statistical Analysis in Climate Research.* Cambridge University Press, 484 pp.